Journal of Engineering Physics and Thermophysics, Vol. 83, No. 5, 2010

COMPARISON OF THE RESULTS OF MODELING CONVECTIVE HEAT TRANSFER IN TURBULENT FLOWS WITH EXPERIMENTAL DATA

A. I. Fomichev

UDC 536.2(075.8):621.1.016

The results of simulation of natural turbulent convection in a square air cavity measuring 0.75 × 0.75 m and having isothermal vertical and highly heat-conducting horizontal walls are compared with the experimental data obtained for this cavity at a Rayleigh number equal to $1.58 \cdot 10^9$. In carrying out numerical investigations, a two-dimensional, low-turbulence, two-parameter k–ε model known as the low-Reynolds-number k–ε turbulence model was used. The results of investigations are presented for the distributions of the velocity and temperature components, as well as local and average values of the Nusselt number. The model was also used in calculating forced turbulent convection in a low-velocity channel with a backward facing step. The results of modeling are compared with experimental data on heat transfer in a turbulent separation flow downstream of the step. In both cases, a satisfactory agreement of the measured values with those predicted by the k–ε turbulence model is obtained.

Keywords: *convective heat transfer, low-Reynolds-number turbulence model, natural and forced convection.*

Introduction. A number of heat-transfer problems of structural thermal physics that are connected with calculation of ventilated and unventilated air interlayers in enclosures, as well as those of transparent structures (windows, glass fronts, garret windows, etc.) must be solved with allowance for the presence, in these constructions, of low-turbulence air flows predominantly induced by natural convection. The data on convective heat-transfer coefficients on the surfaces of structures needed for heat-engineering calculations can be obtained from an experiment, which, however, is rather laborious, intensive, and of specific nature. Another route is numerical simulation of air flows and heat transfer. But here not all of the models of turbulent flows are suitable for modeling natural convection at small Reynolds numbers.

The present investigation was undertaken in order to evaluate the possibility of using one of the variants of the low-Reynolds-number k–ε turbulence model for adequate description of heat transfer and flow characteristics at small Reynolds numbers in the above-specified range of problems. In what follows, for the sake of brevity, this model will be called the k–ε model.

As the main object for comparing the results of modeling, the experimental investigation [1] of natural convection in a square closed air cavity at a Rayleigh number of $1.58 \cdot 10^9$ was selected, which was thoroughly carried out and described in detail in [1]. The second object of modeling selected was the classical problem on separation flow in a channel downstream of a forward-facing step. In this case, the results of modeling were compared with the experimental data of [2] on heat-transfer intensity in the zone of a separated flow.

1. The *k*–ε Model of Turbulence. *Model equations.* The model is based on the low-Reynolds-number k–ε turbulence model with variable coefficients which was described in detail in [3]. The mathematical formulation of the two-dimensional model was made using the Boussinesq approximation for a viscous incompressible fluid, and it includes

the continuity equation:

$$\frac{\partial U}{\partial x} + \frac{\partial V}{\partial y} = 0 ;$$

the momentum equations in the X and Y directions (the Navier–Stokes equations):

Scientific-Research Institute of Structural Physics. 21 Lokomotiv Lane, Moscow, 127238, Russia. Translated from Inzhenerno-Fizicheskii Zhurnal, Vol. 83, No. 5, pp. 907–916, September–October, 2010. Original article submitted August 6, 2009; revision submitted December 9, 2009.

$$\frac{\partial U}{\partial t} + U\frac{\partial U}{\partial x} + V\frac{\partial U}{\partial y} = -\frac{1}{\rho}\frac{\partial P}{\partial x} + \frac{\partial}{\partial x}(\nu + \nu_t)\left(2\frac{\partial U}{\partial x}\right) + \frac{\partial}{\partial y}(\nu + \nu_t)\left(\frac{\partial U}{\partial y} + \frac{\partial V}{\partial x}\right),$$

$$\frac{\partial V}{\partial t} + U\frac{\partial V}{\partial x} + V\frac{\partial V}{\partial y} = -\frac{1}{\rho}\frac{\partial P}{\partial y} + g\beta\,(T - T_m) + \frac{\partial}{\partial y}(\nu + \nu_t)\left(2\frac{\partial V}{\partial y}\right) + \frac{\partial}{\partial x}(\nu + \nu_t)\left(\frac{\partial V}{\partial x} + \frac{\partial U}{\partial y}\right); \quad (1)$$

the energy-transfer equation:

$$\frac{\partial T}{\partial t} + U\frac{\partial T}{\partial x} + V\frac{\partial T}{\partial y} = \frac{\partial}{\partial x}\left(\frac{\nu}{\mathrm{Pr}} + \frac{\nu_t}{\sigma_t}\right)\frac{\partial T}{\partial x} + \frac{\partial}{\partial y}\left(\frac{\nu}{\mathrm{Pr}} + \frac{\nu_t}{\sigma_t}\right)\frac{\partial T}{\partial y}; \quad (2)$$

the equation of transfer of the kinetic energy of turbulent pulsations:

$$\frac{\partial k}{\partial t} + U\frac{\partial k}{\partial x} + V\frac{\partial k}{\partial y} = \frac{\partial}{\partial x}\left(\nu + \frac{\nu_t}{\sigma_k}\right)\frac{\partial k}{\partial x} + \frac{\partial}{\partial y}\left(\nu + \frac{\nu_t}{\sigma_k}\right)\frac{\partial k}{\partial y} + P_k + G_k - \varepsilon; \quad (3)$$

the equation of transfer of the rate of turbulent-energy dissipation:

$$\frac{\partial \varepsilon}{\partial t} + U\frac{\partial \varepsilon}{\partial x} + V\frac{\partial \varepsilon}{\partial y} = \frac{\partial}{\partial x}\left(\nu + \frac{\nu_t}{\sigma_\varepsilon}\right)\frac{\partial \varepsilon}{\partial x} + \frac{\partial}{\partial y}\left(\nu + \frac{\nu_t}{\sigma_\varepsilon}\right)\frac{\partial \varepsilon}{\partial y} + C_1 f_1 \frac{\varepsilon}{k} P_k + C_2 f_2 \frac{\varepsilon^2}{k} + S_\varepsilon. \quad (4)$$

The turbulent viscosity ν_t is expressed in terms of k and ε from the Prandtl–Kolmogorov relation:

$$\nu_t = C_\mu f_\mu \frac{k^2}{\varepsilon}. \quad (5)$$

The generation of turbulence P_k in Eqs. (3) and (4) is modeled by the expression

$$P_k = \nu_t\left[2\left(\frac{\partial U}{\partial x}\right)^2 + 2\left(\frac{\partial V}{\partial x}\right)^2 + \left(\frac{\partial U}{\partial y} + \frac{\partial V}{\partial x}\right)^2\right].$$

The source term G_k in Eq. (3) owing its origin to buoyancy is defined as

$$G_k = -g\beta\frac{\nu_t}{\sigma_t}\frac{\partial T}{\partial y}.$$

The complement of the k–ε model of turbulence with variable coefficients is the source term S_ε in dissipation equation (4) suggested by Yap [4] to correct the turbulence scale near the wall which is defined by the expression

$$S_\varepsilon = 0.83\left(\frac{k^{3/2}}{\varepsilon c_1 y} - 1\right)\left(\frac{k^{3/2}}{\varepsilon c_1 y}\right)^2\frac{\varepsilon^2}{k},$$

where y is the distance from the wall and $c_1 = k^{3/2}/\varepsilon = 2.5$ in the wall zone of constant shear stresses of a flow.

Model constants and functional dependences. In the k–ε model the following constants and dependences are used:

$$C_\mu = 0.09;\ \ \sigma_t = 0.9;\ \ \sigma_k = 1.0;\ \ \sigma_\varepsilon = 1.3;\ \ C_1 = 1.44;\ \ C_2 = 1.92;\ \ f_1 = 1.0;$$

$$f_\mu = \exp\left[-\frac{3.4}{\left(1 + \frac{\mathrm{Re}_t}{50}\right)^2}\right];\ \ f_2 = 1.0 - 0.3\exp\left(-\mathrm{Re}_t^2\right).$$

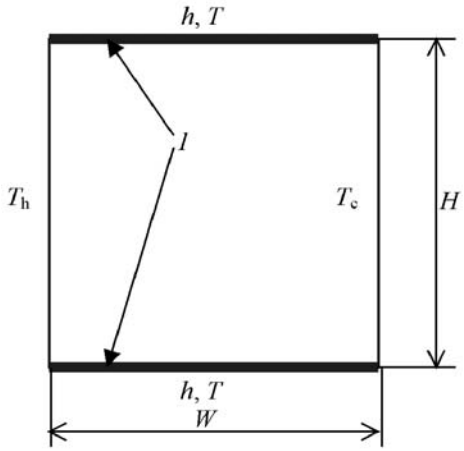

Fig. 1. Geometry and boundary conditions of the model of a cavity: 1, steel sheets of thickness 1.5 mm; $H = W = 0.75$ m; $T_h = 50^oC$, $T_c = 10^oC$, $T = 30^oC$; $h = 1$ W/(m^2·^{o}C).

Boundary conditions. The parameters of the incoming flow (flow velocity or pressure, turbulent kinetic energy k and dissipation of the turbulent kinetic energy ε) are considered known.

Near the wall the following boundary value for k is given:

$$k = 0 ,$$

whereas ε is calculated according to [5] from the formula

$$\varepsilon_w = 2\nu \left(\frac{\partial \sqrt{k}}{\partial n} \right)^2 .$$

Numerical method. To solve the above-given system of two-dimensional equations (1)–(4) in the Cartesian geometry in the presence of conjugate heat transfer, the Flow2D computer program was developed. The program's implicit finite-difference method of discretization of Eqs. (1)–(4) is based on the SIMPLE algorithm developed by Patankar [6]. The resultant system of linear equations is solved by the alternating direction method (the TDMA-method [6]). A stationary solution is obtained by the time-dependent technique with the use of the lower relaxation method. The correctness of the solution procedure was checked by comparing with control results obtained by Davis [7] for laminar convection in a square cavity.

To verify the independence of the results of the grid choice, calculations were carried out for two grids ($39 \times 41 = 1599$ and $55 \times 60 = 3300$ nodes) of the model of a square air cavity. In the nonuniform grid used, such fining of the grid in the boundary layer is employed that there should be no less than five nodes in the inner sublayer of the boundary layer to ensure an adequate display of the physical processes occurring in the wall region. As a result of calculations on two grids, a difference of less than 0.5% was obtained for the mean value of the Nusselt number and the maximum value of velocity and a difference of less than 1% for the maximum value of the Nusselt number on isothermal walls.

2. Modeling of Natural Convection in a Closed Air Cavity. According to the description of the experiment in [1], investigation of natural convection was carried out for a square air cavity measuring 0.75×0.75 m and having heat-conducting horizontal walls made from thermally insulated steel sheets and isothermal vertical walls at a temperature of 50 and 10^{o}C. Outside the cavity, an air temperature equal to 30^{o}C was maintained.

2.1. Geometry and boundary conditions of the cavity model. To compare the results of numerical simulation with the experimental data of [1], the dimensions of the model, its temperature conditions, and the properties of materials were assigned as close to those described in [1] as possible. The geometry of the model and its boundary conditions are presented in Fig. 1. The heat insulation of the horizontal walls is modeled by the heat-transfer coefficient $h = 1.0$ W/(m^2·^{o}C). The thermal conductivity of stainless steel was taken equal to 17.0 W/(m·^{o}C).

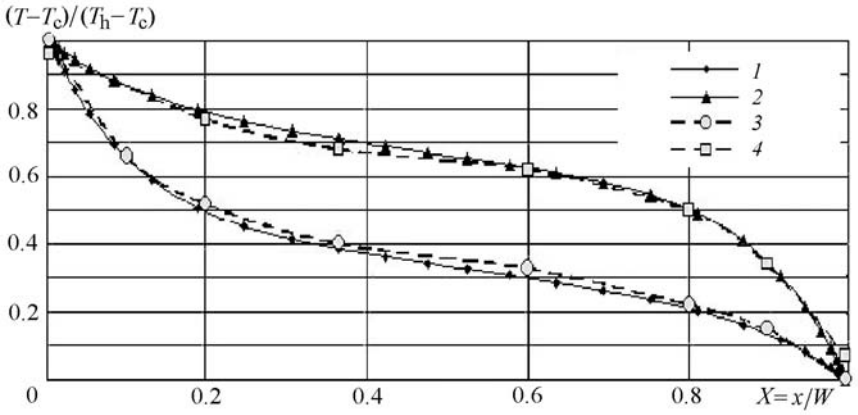

Fig. 2. Comparison between predicted and experimental distributions of the relative temperature along the horizontal walls of the cavity: 1) lower wall, prediction; 2) upper wall, prediction; 3) lower wall, experiment; 4) upper wall, experiment.

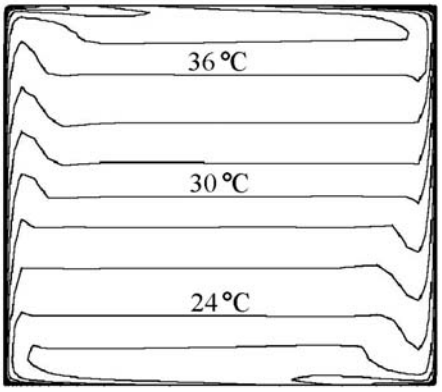

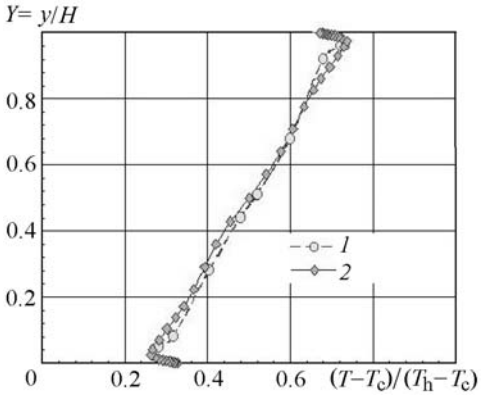

Fig. 3. Temperature distribution on the cavity model.

Fig. 4. Comparison between predicted and experimental distributions of temperature along the vertical passing through the middle of the cavity bottom: 1) experiment [1]; 2) k–ε model.

As a result of calculations, a temperature distribution along the horizontal walls close to the values measured experimentally was obtained (Fig. 2). Calculations of the Rayleigh number based on the properties of air given in [8] for a mean temperature of the cavity of 30°C gave the value Ra = $1.62\cdot10^9$. These very properties of air were used in modeling convection. In the experiment in [1], the Rayleigh number was estimated equal to $1.58\cdot10^9$.

2.2. Temperature distribution. The temperature field of the cavity, is shown in Fig. 3 in the form of a set of isotherms. In the central zone of the cavity, air stratification is observed. The predicted and measured temperature distributions in the vertical section at the center of the cavity are given in Fig. 4. Vertically the temperature changes by a law close to the linear one. The obtained values of the nondimensional temperature at the center of the cavity and the stratification parameter S_p defined by the relation

$$S_p = \frac{H}{T_h - T_c}\frac{\partial T}{\partial y}\bigg|_{x/W=0.5;y/H=0.5}$$

are compared in Table 1.

The temperature profiles near the hot wall in the middle of the cavity height obtained in the present investigation and in [1] are shown in Fig. 5. The coincidence of the profiles in the inner part of the boundary layer can be

TABLE 1. Parameters of the Temperature Distribution at the Center of the Square Cavity

Source of data	$(T - T_c)/(T_h - T_c)$	S_p
Experiment [1]	0.514	0.50
k–ε model	0.50	0.46

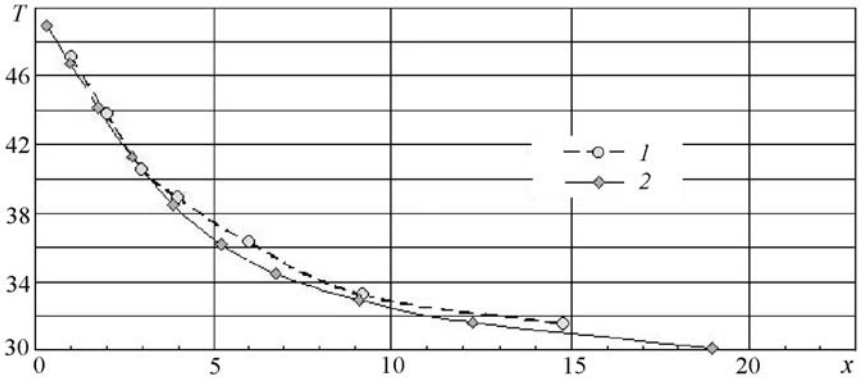

Fig. 5. Comparison between predicted and experimental temperature profiles near the hot wall in the middle of the cavity height: 1) experiment [1]; 2) k–ε model. T, °C; x, mm.

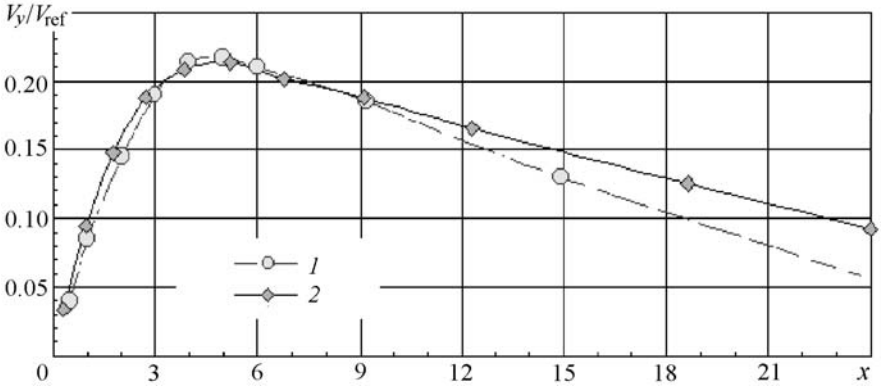

Fig. 6. Comparison between predicted and experimental velocity profiles near the hot wall (V_{ref} = 1.038 m/s: 1) experiment [1]; 2) k–ε model. x, mm.

noted. The angles of inclination of lines in the laminar sublayer of the boundary layer are practically the same, pointing to the closeness of the heat-flux-density values at the boundary.

2.3. Velocity distribution. Figure 6 presents a comparison of the calculated velocity profile near the hot wall with the velocity profile obtained experimentally in [1]. The value of the maximum vertical velocity obtained by modeling is 3% smaller than the experimental value. On the whole, the k–ε model predicts changes of velocity in the inner part of the boundary layer close to the experimental ones, as well as the position of the velocity peak relative to the wall, which confirms that the estimations of the wall shear stresses obtained with the aid of the numerical model are adequate to the experiment. However, the width of the boundary layer predicted by this model is larger than that obtained in the experiment.

A comparison of the profiles of the horizontal velocity component in the vertical section in the middle of the cavity is presented in Fig. 7. The maximum velocity in a horizontal boundary layer obtained in the experiment is 12% higher than the maximum velocity predicted by the k–ε model. The experimental data also show the presence of a backflow along the outside edge of the horizontal boundary layer, which is not predicted by the k–ε model.

2.4. Heat fluxes. A comparison of the distributions of the Nusselt number along the hot vertical wall is shown in Fig. 8. The Nusselt number is determined from the equality

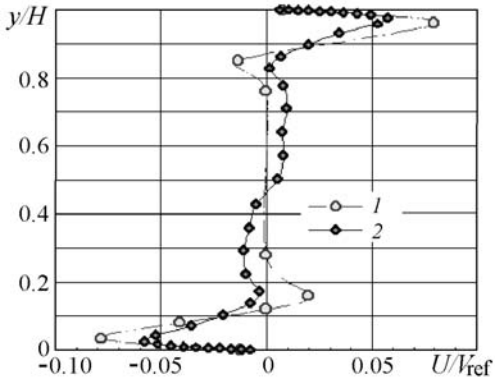

Fig. 7. Comparison between predicted and experimental profiles of the horizontal velocity component on the vertical in the middle of the cavity: 1) experiment [1]; 2) k–ε model.

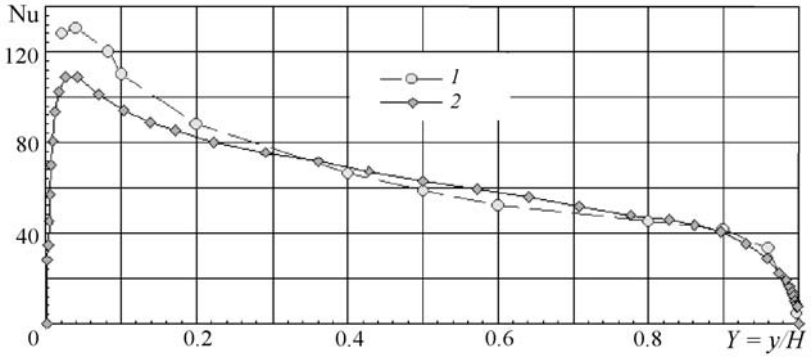

Fig. 8. Comparison between predicted and experimental distributions of the local Nusselt number along the hot vertical wall of the cavity: 1) experiment [1]; 2) k–ε model.

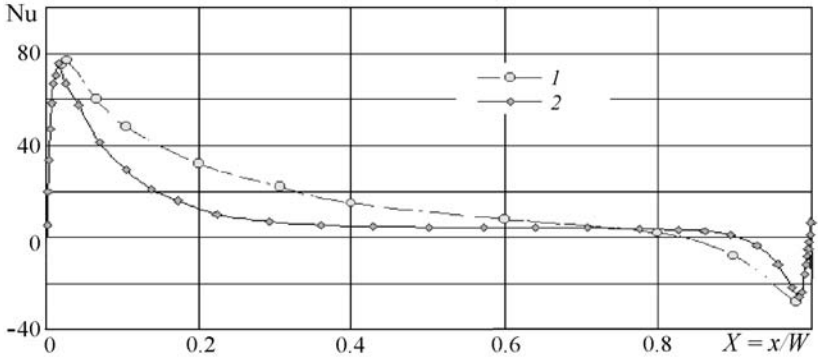

Fig. 9. Comparison between predicted and experimental distributions of the local Nusselt number along the surface of the cavity bottom: 1) experiment [1]; 2) k–ε model.

$$\mathrm{Nu} = \frac{q}{\dfrac{\lambda_g (T_h - T_c)}{W}}.$$

The turbulent model yields a maximum value of the Nusselt number which is 15% smaller than that obtained in the experiment; however, on the whole the agreement between the theoretical and experimental distributions is satisfactory. Figure 9 presents a comparison between the theoretical and experimental distributions of the Nusselt number

TABLE 2. Comparison between Predicted and Experimental Mean Values of the Nusselt Number

Source of data	Nu			Error relative to experiment, %
	hot wall	cold wall	mean value for the cavity	
Experiment [1]	64.0	65.3	64.5	—
k–ε model	63.94	63.88	63.9	–0.9

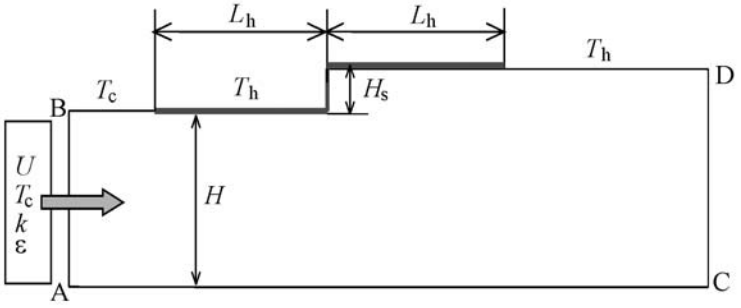

Fig. 10. Schematic of the model of the channel with a step: AB, flow entry; CD, flow exit; L_h = 305 mm; H_s = 6.4 mm; H = 0.2 m; U = 1.65 m/s; T_h = 18°C, T_c = 0°C.

along the surface of the cavity bottom, where the direction of the heat flux is changed. Here, the picture is different: the maximum values of the Nusselt number obtained experimentally and in modeling practically coincide, but over the remaining part of the surface the k–ε model predicts smaller values of the Nusselt number than those obtained experimentally.

Table 2 compares mean values of the Nusselt number on isothermal walls of the cavity. It is seen from the table that the predicted values are very close to those obtained experimentally.

2.5. Turbulent kinetic energy. The values of the turbulent kinetic energy predicted by the k–ε model are on the average 10–15% less than those obtained experimentally. According to [1], the maximum value of the turbulent kinetic energy was equal to $3.5 \cdot 10^{-3}$ for the cold wall and $4.5 \cdot 10^{-3}$ m^2/s^2 for the hot wall. The numerical simulation yields values of $3.1 \cdot 10^{-3}$ and $3.6 \cdot 10^{-3}$ m^2/s^2, respectively.

3. Modeling of a Turbulent Flow in a Channel with a Step. Below, the results of modeling are compared with experimental investigations [2] of heat transfer in a turbulent separation flow in a low-velocity channel downstream of a forward-facing step. The temperature distribution and the local values of the heat-transfer coefficient in the zone of a separation flow were obtained in an experiment by means of a Mach–Zehnder interferometer. The error of temperature measurements was estimated within ±7%. Of the three values of the inlet flow velocity used in the experiment, in the present work only the flow with a least velocity of 1.65 m/s is modeled.

In such problems it is of interest to determine the position of the critical point at the boundary between the recirculation zone and the main flow, as well as the maximum value of the heat-transfer coefficient which is usually observed near this point. The position of the critical point is determined as the distance from the step expressed in units equal to the step height. In the experiment in [2], the distance of the critical point from the step is estimated as 4.5 times the step height.

3.1. Geometry and boundary conditions of the model of a channel. The dimensions and boundary conditions of the numerical model correspond to the description of the experimental setup consisting of a rectangular section of a low-velocity channel, on the upper wall of which a model of a step is installed; the step has temperature excessive relative to that of the inlet flow. The schematic representation of the geometry and boundary conditions of the model is given in Fig. 10.

At the inlet boundary AB the flow parameters are given: U, T_h, k, and ε. At the inlet flow velocity U = 1.65 m/s, for the characteristic dimension corresponding to the height of the step the Reynolds number is equal to 800. In [2] no estimate is given for the turbulence level of the inlet flow; it is only known that a band vortex generator was used in the boundary layer of the flow upstream of the step model. To estimate the dependence of

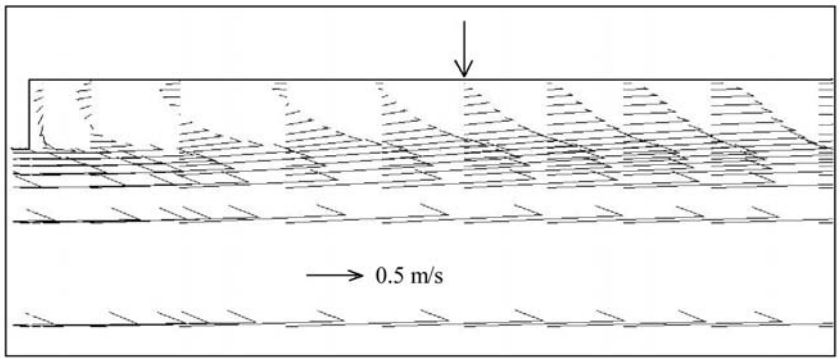

Fig. 11. Velocity field. The arrow indicates the position of the critical point, where the recirculation zone downstream of the step terminates.

the results of numerical simulation on the turbulence level two calculations were carried out for a low intensity of

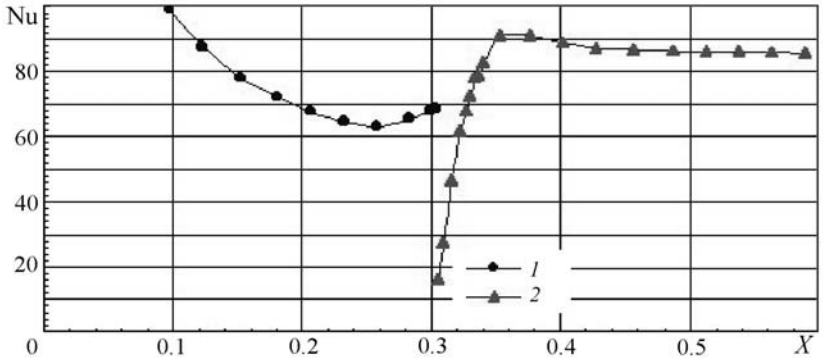

Fig. 12. Distribution of the Nusselt number along the hot wall of the channel: 1) the value of Nu upstream of the step; 2) the value of Nu downstream of the step. X, m.

turbulence of the inlet flow at the turbulent kinetic energy $k = 1.0 \cdot 10^{-4}$ m^2/s^2 and at $k = 2.3 \cdot 10^{-4}$ m^2/s^2. The kinetic-energy dissipation for the indicated values of k and assigned relative turbulent viscosity ν_t/ν was calculated from Eq. (5) and amounted to $2.2 \cdot 10^{-5}$ and $8.4 \cdot 10^{-5}$ m^2/s^3 at $\nu_t/\nu = 3$ and 4, respectively. At the exit boundary CD the condition of zero gradients of the variables U, T, k, and ε along the flow direction is satisfied.

3.2. Results and analysis. The results of simulation were compared with experimental data by two indices: the distance from the step to the critical point normalized by the step height and the maximum value of the heat-transfer coefficient along the flow downstream of the step normalized by the value of the heat-transfer coefficient directly upstream of the step. The value of the first index obtained in the experiment is equal to 4.5. The value of the second index turned out to be equal to 1.2 and is essentially an averaged value obtained experimentally for three velocities of an inlet flow. From the experimental data it follows directly that for a velocity of 1.65 m/s this value is also equal to 1.25.

From the results of simulation, the distance from the step to the critical point was determined from the condition of vanishing of the horizontal velocity component near the wall. The distance from the step to the critical point was equal to 4.95. For a laminar regime of flow, under other conditions being equal, this distance amounts to 9.5. The resulting vector field of velocities in the zone of the channel downstream of the step is shown in Fig. 11.

Figure 12 presents the obtained distribution of the local Nusselt number along the channel wall with a step. At the point where the wall geometry is altered (a step), a jump in the values of the Nusselt number occurs. The ratio of the maximum value of the Nusselt number downstream of the step to the value of the Nusselt number directly upstream of the step corresponds to the ratio of the values of the heat-transfer coefficients in the indicated regions and is equal to 1.33, which is 6.4% higher than that obtained experimentally.

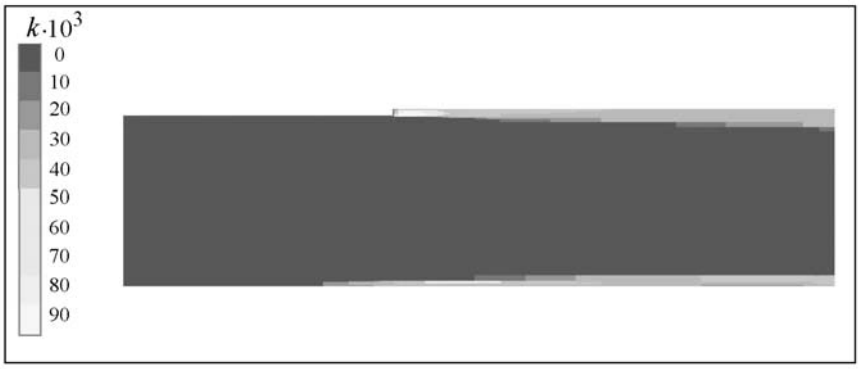

Fig. 13. Distribution of the turbulent kinetic energy $k \cdot 10^3$ m^2/s^2 in the model of the channel. k, m^2/s^2.

Figure 13 presents the distribution of the turbulent kinetic energy predicted by the k–ε model for a channel. A maximum value of the turbulent kinetic energy is observed in the zone of recirculation downstream of the step and is equal to 0.085 m^2/s^2. This value does not change with the turbulence level of the inlet flow within the values indicated in Sec. 3.1. The same is true of the indices compared with the experiment. However, 3.5% increase in maximum values of the Nusselt number upstream of the step and downstream of it is noted, with the character of the distribution of the Nusselt number being practically preserved. Thus, the obtained values of normalized indices are independent of the turbulence level for the selected limits of the turbulent parameters of the inlet flow.

Conclusions. The low-Reynolds-number, two-dimensional, two-parameter k–ε turbulence model has been applied for predicting convective heat transfer in turbulent flows at small Reynolds numbers in a closed square air cavity and in a channel with a step.

In the first problem, the results of simulation were compared with the experimental data of [1] on the investigation of natural convection at a Rayleigh number of $1.58 \cdot 10^9$ in a square closed air cavity measuring 0.75×0.75 m and having highly heat-conducting horizontal walls and isothermal vertical walls at a temperature of 50 and 10°C. The comparison has shown that on the whole the low-Reynolds-number k–ε turbulence model predicts the characteristics of a flow, heat transfer in it, and its turbulent parameters in good correspondence with experimental data. Thus, the difference between the predicted and experimental values of the average Nusselt number for a vertical isothermal wall amounted to 0.9%, whereas the difference between maximum values of the vertical velocity at a height of $y = 0.5H$ amounted to no more than 3%. In a horizontal boundary layer adjacent to a nonisothermal wall, a great discrepancy between maximum values of the horizontal velocity amounting to 12% was obtained. Maximum values of the turbulent kinetic energy predicted by the numerical model are equal to $3.1 \cdot 10^{-3}$ and $3.6 \cdot 10^{-3}$ m^2/s^2 as against the experimental values of $3.5 \cdot 10^{-3}$ and $4.5 \cdot 10^{-3}$ m^2/s^2 for the hot and cold walls, respectively.

In the second problem, the results of simulation are compared with experimental investigations [2] of convective heat transfer in a turbulent separation flow in a low-velocity channel (U = 1.65 m/s) downstream of a forward-facing step at a Reynolds number equal to 800. The independence of the results of numerical simulation of the level of turbulence at a turbulent kinetic energy of the inlet flow in the range from $k = 1.0 \cdot 10^{-4}$ m^2/s^2 to $k = 2.3 \cdot 10^{-4}$ m^2/s^2 has been revealed. The results of modeling were compared with experimental data by two indices: the distance from the step to the critical point normalized by the step height and the maximum value of the heat-transfer coefficient downstream of the step normalized by the value of the heat-transfer coefficient directly upstream of the step. According to the experimental data, these indices are equal to 4.5 and 1.25, respectively. The simulation gave values of 4.95 and 1.33, which are 10 and 6.4% higher.

The results obtained show that the low-Reynolds-number k–ε turbulence model presented in this work can be recommended as a computational instrument for predicting the characteristics of heat transfer and of air flows at small Reynolds numbers in such engineering problems as the calculation of air interlayers in the enclosures of buildings or determination of the heat-transfer coefficients on the surfaces of transparent constructions.

NOTATION

C_μ, C_1, C_2, constants in Eqs. (4) and (5); c_1, coefficient of linear scale of turbulence; f_μ, f_1, f_2, damping functions in Eqs. (4) and (5); g, gravitational acceleration, m/s^2; G_k, source term in Eq. (3); h, heat-transfer coefficient, W/(m^2·^{o}C); H, height of a cavity or channel. m; H_s, height of a step, mm; k, turbulent kinetic energy, m^2/s^2; L_h, length of the heated portion of the channel wall, mm; Nu, Nusselt number; n, normal to the nearest wall, m; P, pressure, Pa; P_k, turbulence generation in Eqs. (3) and (4); Pr = ν/α, Prandtl number; q, local heat-flux density, W/m^2; Ra = Pr$g\beta(T_h - T_c)H^3/\nu^2$, Rayleigh number; $\mathrm{Re}_t = k^2/(\nu\varepsilon)$, turbulent Reynolds number; S_ε, source term in dissipation equation (4); S_p, stratification parameter; t, time, s; T, temperature, ^{o}C; T_c, temperature of the cold wall, ^{o}C; T_h, temperature of the hot wall, ^{o}C; T_m, mean temperature of the computational domain, ^{o}C; $(T - T_c)/(T_h - T_c)$, relative temperature; U, horizontal velocity component, m/s; V, vertical velocity component, m/s; $V_{ref} = [g\beta(T_h - T_c)]^{1/2}$, reference velocity, m/s; W, cavity width, m; x, horizontal coordinate, m; y, vertical coordinate, m; X, Y, relative distance along the coordinates x and y; α, thermal diffusivity, m^2/s; β, coefficient of thermal expansion, 1/^{o}C; λ_g, thermal conductivity of a gas, m/s; W/(m·^{o}C); ε, dissipation of turbulent kinetic energy, m^2/s^3; ε_w, value of dissipation at the boundary near the wall; μ, molecular viscosity; ν, kinematic viscosity, m^2/s; ν_t, turbulent viscosity, m^2/s; ρ, density, kg/m^3; σ_k, σ_t, σ_ε, turbulent Schmidt numbers (constants). Subscripts: c, cold; g, gas; h, hot; k, kinetic; l, length; m, mean; p, parameter; ref, reference; t, turbulent; w, boundary value near the wall; s, step.

REFERENCES

1. Y. S. Tian and T. G. Karyiannis, Low turbulence natural convection in an air filled square cavity. Part I: The thermal and fluid flow fields; Part II: The turbulence quantities, *Int. J. Heat Mass Transfer*, **43**, 849–884 (2000).
2. W. Aung and R. J. Goldstein, Heat transfer in turbulent separated flow downstream of a rearward-facing step, *Israel J. Technology*, **10**, Nos. 1–2, 35–41 (1972).
3. T. J. Heindel, S. Ramadhyani, and F. P. Incropera, Assessment of turbulence models for natural convection in an enclosure, *Numer. Heat Transfer*, Part B, **26**, 147–172 (1994).
4. C. Yap, *Turbulent Heat and Momentum Transfer in Recirculating and Impinging Flows: Ph.D Thesis*, Faculty of Technology, University of Manchester (1987).
5. W. M. To and J. A. C. Humphrey, Numerical simulation of buoyant, turbulent flow-1. Free convection along a heated, vertical, flat plate, *Int. J. Heat Mass Transfer*, **29**, 573–592 (1986).
6. S. Patankar, *Numerical Methods for Solving Problems of Heat Transfer and Fluid Dynamics* [Russian translation], Énergoatomizdat, Moscow (1984).
7. G. De Vahl Davis, Natural convection of air in a square cavity: a bench mark numerical solution, *Int. J. Numer. Meth. Fluids*, **3**, 249–264 (1986).
8. ISO 15099. *Thermal Performance of Windows, Doors and Shading Devices — Detailed Calculations*, International Standard (2003).